



Published in final edited form as:

*Magn Reson Med.* 2023 July ; 90(1): 211–221. doi:10.1002/mrm.29618.

## Vascular Space Occupancy Asymmetric Spin Echo (VASO-ASE) for Non-invasive Quantification of Cerebral Oxygen Extraction Fraction

Spencer L. Waddle<sup>1</sup>, Maria Garza<sup>1</sup>, Chunwei Ying<sup>2</sup>, L. Taylor Davis<sup>3</sup>, Lori C. Jordan<sup>1,3,4</sup>, Hongyu An<sup>2</sup>, Manus J. Donahue<sup>1,5,\*</sup>

<sup>1</sup>Department of Neurology, Vanderbilt University Medical Center, Nashville, TN, USA

<sup>2</sup>Mallinckrodt Institute of Radiology, Washington University School of Medicine, St. Louis, MO, USA

<sup>3</sup>Department of Radiology and Radiological Sciences, Vanderbilt University Medical Center, Nashville, TN, USA

<sup>4</sup>Department of Pediatrics, Vanderbilt University Medical Center, Nashville, TN, USA

<sup>5</sup>Department of Psychiatry and Behavioral Sciences, Vanderbilt University Medical Center, Nashville, TN, USA

### Abstract

**Purpose:** Asymmetric Spin Echo (ASE) MRI is a method for measuring regional oxygen extraction fraction (OEF), however, extravascular tissue models have been shown to underestimate OEF. The hypothesis investigated here is that the addition of a vascular-space-occupancy (VASO) pre-pulse will more fully suppress blood water signal and provide global OEF values more consistent with physiological expectation and <sup>15</sup>O PET-validated *T*<sub>2</sub>-relaxation-under-spin-tagging (TRUST) OEF measures.

**Methods:** Healthy adults (n=14; age=27.7±5.2 years; sex=7/7 male/female) were scanned at 3.0T. Multi-echo ASE without inter-readout refocusing (ASE<sub>RF-</sub>), multi-echo ASE with inter-readout refocusing (ASE<sub>RF+</sub>), and single-echo VASO-ASE were acquired twice each with common spatial resolution=3.4x3.4x3.0 mm and τ=0-20 ms (interval=0.5 ms). TRUST was acquired twice sequentially for independent global OEF assessment (τ<sub>CPMG</sub>=10 ms, effective echo times=0, 40, 80, and 160 ms, spatial resolution=3.4x3.4x5 mm). OEF intraclass-correlation-coefficients (ICC), summary statistics, and group-wise differences were assessed (Wilcoxon Rank-Sum; significance: two-sided *p*<0.05).

**Results:** ASE<sub>RF+</sub> (OEF=36.8±1.9%) and VASO-ASE (OEF=34.4±2.3%) produced OEF values similar to TRUST (OEF=36.5±4.6%; human calibration model; OEF=32.7±4.9%; bovine calibration model), however, ASE<sub>RF-</sub> yielded lower OEF (OEF=26.1±1.0%; *p*<0.01) relative to TRUST. VASO-ASE (ICC=0.61) yielded lower ICC compared to other ASE variants (ICC>0.89).

\*Corresponding Author Manus J Donahue, MBA, PhD, Department of Neurology, Vanderbilt University Medical Center, 1500 21<sup>st</sup> Ave South, Suite 2600, Nashville, TN 37232 USA, mj.donahue@vumc.org, Tel: 615.322.8350.

**Conclusion:** VASO-ASE and TRUST provide similar OEF values, however, VASO-ASE spatial coverage and repeatability improvements are required.

### Keywords

Asymmetric Spin Echo; Oxygen Extraction Fraction; VASO; qBOLD; T2-Relaxation-Under-Spin-Tagging

## Introduction

Quantitative measurements of cerebral oxygen extraction fraction (OEF), or the ratio of oxygen consumed by brain tissue to that which is delivered, provide valuable functional information regarding tissue health in patients with cerebrovascular and neurodegenerative diseases<sup>1-4</sup>.

OEF can be quantified using <sup>15</sup>O-PET<sup>1,5,6</sup>, however, this technique requires ionizing radiation, arterial blood sampling, and an on-site cyclotron due to the short 122s half-life of <sup>15</sup>O, rendering it impractical as a generalizable diagnostic tool. Alternative *T*<sub>2</sub>-relaxation-under-spin-tagging (TRUST)<sup>7</sup> and Asymmetric Spin Echo (ASE)<sup>8</sup> methods have been proposed for measuring OEF non-invasively *in vivo* using MRI.

TRUST has demonstrated high intrascan repeatability (Intrascan Coefficient-of-Variation=3.84±1.44%)<sup>9</sup> and consistency with gold-standard PET<sup>10</sup> in healthy adults (Intraclass Correlation Coefficient=0.90)<sup>11</sup>, and has been successfully implemented in patients with cerebrovascular and neurodegenerative diseases<sup>12-14</sup>. However, TRUST is restricted to a whole-brain measure of OEF and does not provide spatial information.

ASE utilizes a spin echo variant, generally paired with a fast echo planar imaging (EPI) readout. Here, the location of the spin echo refocusing pulse is incrementally shifted, while the readout location is retained; images acquired at each refocusing offset, or  $\tau$ , provide voxel-wise  $R_2'$  weighting.  $R_2'$  is influenced by susceptibility from surrounding paramagnetic deoxy-hemoglobin, as well as other sources of susceptibility. To quantify blood oxygenation, a model is frequently applied which relates susceptibility effects from extravascular tissue to blood oxygenation and venous cerebral blood volume (vCBV). This model accounts for extravascular signal dephasing under the assumption that intravascular contributions are negligible. This assumption can be made approximately valid by introducing dephasing gradients<sup>8</sup>, however, such signal suppression is dependent on gradient orientation and strength relative to blood flow velocity and direction, and therefore this approach can have variable effects in voxels with different blood kinetics and vascular orientations. Healthy whole-brain OEF values are generally reported as 31-44% depending on method used, and CBV as 0.02-0.03 ml blood / 100g tissue, with vCBV being approximately 70% of total CBV<sup>15</sup>. However, as a result of incomplete blood water nulling, diffusion, and extravascular sources of susceptibility, the ASE method may overestimate vCBV and underestimate OEF, frequently reporting vCBV values of 0.04-0.06 ml blood / 100g tissue and OEF values of 20-30%<sup>8,16,17</sup>.

Alternatively, the longitudinal component of blood water magnetization can be suppressed using principles of inversion recovery with the vascular-space-occupancy (VASO) technique<sup>18-21</sup>. VASO uses an inversion pre-pulse with an inversion time (TI) chosen to null the longitudinal component of blood water magnetization at the time of excitation. A similar module may be played before the ASE sequence in a proposed VASO-ASE approach.

Here, sequential measurements are acquired with VASO-ASE, along with more conventional dual-echo ASE methods without VASO blood water nulling, and we compare all variants to whole-brain OEF recorded from TRUST-MRI, which has been validated in healthy adults against historical gold-standard <sup>15</sup>O-PET OEF<sup>11</sup>. The hypothesis to be investigated is that VASO-ASE, relative to other ASE variants, will provide OEF values more consistent with TRUST OEF values.

## Methods

### Participants

Healthy, adult participants provided informed, written consent in accordance with the Vanderbilt University Institutional Review Board and the Declaration of Helsinki. Inclusion criteria consisted of no history of cerebrovascular disease, anemia, psychosis, or neurological disorder including but not limited to prior overt stroke, sickle cell anemia, schizophrenia, bipolar disorder, Alzheimer's disease, Parkinson's disease, or multiple sclerosis.

### Acquisition

All participants underwent an MRI protocol on a Philips (Philips Healthcare, Best, The Netherlands) Ingenia 3.0T that consisted of non-contrasted anatomical imaging, to ensure inclusion criteria were met, complemented with ASE and TRUST sequences. To evaluate repeatability, all OEF scan variants were repeated once in each participant in the same approximately 40-minute scan session without repositioning.

**Anatomical Imaging.**—All participants underwent axial 2D Fluid-Attenuation-Inversion-Recovery (FLAIR; TR/TI/TE=11000/2800/120 ms; spatial resolution=0.96x1.29x4.00 mm) and 3D  $T_1$ -weighted MPRAGE (TR/TE=8.2/3.7; spatial resolution=1.0x1.0x1.0 mm) MRI.

### Asymmetric Spin Echo (ASE).

Three ASE variants were performed without parallel imaging using the following conserved parameters: TR=4400 ms, TE<sub>1</sub>=64 ms, spatial resolution=3.4x3.4x3.0 mm, slices=13, slice gap=3 mm. Slices in each TR was acquired with equidistant temporal slice spacing and interleaved spatial acquisition. Fat saturation was accomplished with a spectral pre-saturation inversion recovery (SPIR) pulse. Peripheral Nerve Stimulation (PNS) and gradient modes were both set to high (Max B<sub>1</sub>=13.5  $\mu$ T, max gradient strength=22.5 mT/m, max slew rate=180 mT/m/ms). For echo shifting, the refocusing pulse was shifted temporally from TE<sub>1</sub>/2 by a value,  $\tau$ . The  $\tau$  value ranged from 0 to 20 ms and images were acquired in intervals of 0.5 ms, resulting in 41 total values, each acquired in a separate TR. These images with different  $\tau$  were randomized in acquisition order to reduce systematic

artifacts from scanner drift. Each scan was repeated once for a total of two acquisitions per participant for each of three ASE variants,

- i. ASE<sub>RF-</sub>: This method was designed to reproduce the sequence most frequently performed in neuroimaging applications of ASE<sup>22-24</sup>. A dual-echo (TE<sub>2</sub>=107 ms) multi-slice ASE sequence without a 180-degree refocusing pulse between the first and second echoes to increase overall susceptibility weighting (Figure 1a),
- ii. ASE<sub>RF+</sub>: A similar dual-echo (TE<sub>2</sub>=107 ms) multi-slice ASE sequence with a 180-degree refocusing pulse between the first and second read-outs (Figure 1b), and
- iii. Vascular-space-occupancy ASE (VASO-ASE): A single-slice, single-echo ASE sequence with TI=1039 ms (Figure 1c)<sup>18</sup>.

Geometry and readout parameters were matched between variants, however, the VASO-ASE method included only a single echo owing to lower SNR, given residual gray and white matter magnetization of only 10-20% at the blood water inversion time prescribed. The second readout in ASE<sub>RF-</sub> provides an image with a different R<sub>2</sub>' weighting, while the ASE<sub>RF+</sub> second readout has the same R<sub>2</sub>' weighting as the first. To investigate potential differences between VASO-ASE and other ASE variants that may be caused by variation in slice or echo number, we analyzed dual-echo and the first echo only of non-VASO-ASE variants to understand whether any differences were attributable to the blood nulling pre-pulse or the dual-echo approach. The steady-state solution to the Bloch equation for longitudinal magnetization (M<sub>z</sub>) following inversion recovery is<sup>19</sup>:

$$M_z(TI) = M_0 \cdot (1 - 2e^{-TI/T_{1,b}} + e^{-TR/T_{1,b}}) = 0. \quad [\text{Eq 1}]$$

Using  $T_1$  of blood at 3.0T ( $T_{1,b}$ )=1664 ms<sup>25</sup>, and the prescribed TR=4400 ms, TI for blood water nulling is calculated as 1039 ms. This TI yields a residual blood water M<sub>z</sub>/M<sub>0</sub> < 0.001, but white matter ( $T_1$ =800 ms) and gray matter ( $T_1$ =1200 ms) residual M<sub>z</sub>/M<sub>0</sub> of 0.458 and 0.184, respectively.

**T<sub>2</sub>-Relaxation-Under-Spin-Tagging (TRUST).**—TRUST was acquired and repeated once for measuring whole-brain OEF<sup>7,10</sup>. Here, post-label delay=1022 ms, interpulse gap (τ<sub>CPMG</sub>)=10 ms, and four effective TEs (eTE)=0 ms, 40 ms, 80 ms, and 160 ms (three averages per eTE) were utilized. Arterial oxygen saturation (Y<sub>a</sub>) was simultaneously recorded during TRUST with an MRI-compatible pulse-oximeter. The spatial resolution of TRUST was 3.4x3.4x5.0 mm, optimized in prior work<sup>10</sup>. TRUST records blood oxygenation from a single region in the sagittal sinus approximately 20 mm superior to the torcula, and thus it is not relevant to match spatial resolution with ASE.

## Image Analysis and Processing

**Anatomical imaging.**—FLAIR and T<sub>1</sub>-weighted images were evaluated to ensure that radiological inclusion criteria were met.

**ASE.**—Acquired images were spatially smoothed using a 3-by-3-voxel kernel (10.32 x 10.32 mm) prior to processing to improve SNR for fitting. Calculation of physiological parameters has been described previously<sup>8,26</sup> and we followed the same procedure. Briefly, a susceptibility model, which relates OEF,  $R_2'$  and vCBV<sup>27</sup>, was applied to signal obtained as a function of  $\tau$ . First, a linear model was fit to logarithmic long- $\tau$  values ( $\tau > 10$  ms), simultaneously for both the first and second echo, which yielded the relaxation rate,  $R_2'$ . Logarithmic short- $\tau$  ( $\tau \leq 10$  ms) values were then fit to a quadratic model, which yielded vCBV. The signal equation for the second echo was similar to the first, however for the second echo, a term for signal decay between the readouts was included;  $R_2^*$  decay for ASE<sub>RF-</sub>, and  $R_2$  decay for ASE<sub>RF+</sub>. Eq 2 was applied to quantify OEF:

$$OEF = \frac{R_2'}{\gamma \cdot vCBV \cdot \frac{4}{3} \cdot \pi \cdot \Delta\chi_0 \cdot Hct \cdot B_0}, \quad [\text{Eq 2}]$$

where  $\gamma$  is gyromagnetic ratio in radians/(s\*T),  $\chi_0$  is the human blood susceptibility difference between fully oxygenated and fully deoxygenated blood per unit hematocrit<sup>28</sup>= $0.18 \times 10^{-6}$ , Hct is the small-vessel hematocrit estimated as 35.7% (85% of a large vessel hematocrit of 42%)<sup>8</sup>, and  $B_0=3.0T$ .

Mean values were acquired by co-registering processed parameter maps to a standard Montreal Neurological Institute (MNI) 1 mm brain atlas using FSL-FLIRT<sup>29</sup> with  $T_1$  as an intermediary template, and measuring mean values in segmented white matter. Given that gray matter voxels may contain partial-volume effects from cortical vessels and neighboring CSF at this typical spatial resolution, analysis was focused on white matter, which is also the location of most ischemic lesions. Following co-registration to the atlas, maps were spatially smoothed at 9x9 mm to render final maps representative of the spatial resolution at which fitting was applied.

**TRUST.**—We followed previously-published, standard procedures to quantify whole-brain OEF from TRUST<sup>7,10,30</sup>. OEF was calculated as the fractional difference of arterial oxygen saturation, measured with pulse-oximetry, and venous oxygen saturation, measured with TRUST. TRUST images were pair-wise subtracted, averaged across three measurements, and an empirical model calibrated in human HbAA blood and more complete model calibrated in bovine blood were both applied separately for completeness<sup>10,31</sup>.

## Statistical Analysis

ASE variants were compared to assess repeatability and correspondence of quantified OEF with TRUST. First, intraclass correlation coefficients (ICC) were calculated between repeated measurements of TRUST and each ASE variant, where ICC=0.50-0.75 was considered moderate, ICC=0.75-0.90 was considered good, and ICC>0.90 was considered excellent repeatability<sup>32</sup>. Repeated measures were visualized as Bland-Altman plots and scatter plots, for which slope of a linear fit is provided along with Pearson's R values and corresponding p-values. All group-wise comparisons were performed with a Wilcoxon Rank-Sum test with significance threshold  $p < 0.05$  (Bonferonni correction to  $p=0.013$  for

four methods used to calculate OEF). Values are reported as both mean±standard deviation as well as median, first quartile (Q1), and third quartile (Q3).

## Results

### Participants

This study included 14 participants scanned between March 1<sup>st</sup> and August 8<sup>th</sup> of 2021. Participants were 27.7±5.2 years old (range=21-42 years), and 50% male and 50% female (Table 1). Racial makeup of the cohort was 11/14 (79%) White, 2/14 (14%) Asian, and 1/14 (7%) Black. All participants met stated inclusion criteria and were without radiological evidence of cerebrovascular or neurodegenerative disease.

### Repeatability

Repeatability measures were taken for each ASE variant (Figure 2 and Supporting Information Table S1). Repeatability was similar and excellent for TRUST (ICC=0.98), ASE<sub>RF-</sub> (ICC=0.91), and ASE<sub>RF+</sub> (ICC=0.89), however, moderate for VASO-ASE (ICC=0.61).

### OEF Metrics

Representative quantitative OEF, vCBV, and R<sub>2</sub>' maps for each ASE variant are shown in Figure 3, and acquired ASE images are shown in Supporting Information Figure S1. When dual-echo versions of ASE were compared to VASO-ASE (a single echo sequence), ASE<sub>RF+</sub> (OEF=36.8±1.9%; median=36.2%, Q1=35.8%, Q3=37.7%) and VASO-ASE (OEF=34.4±2.3%, median=34.0, Q1=32.8, Q3=35.3) produced OEF values that were not significantly different (ASE<sub>RF+</sub>: p=0.35, VASO-ASE: p=0.19) from TRUST using the HbAA model (OEF=36.5±4.6%, median=35.4, Q1=33.2%, Q3=39.4%). However, ASE<sub>RF-</sub> produced values (OEF=26.1±1.0%, median=26.2, Q1=25.7%, Q3=26.8%) that were significantly lower (p<0.01). With the bovine blood calibration model applied to TRUST data (OEF=32.7±4.9%; median=31.5%, Q1=29.3%, Q3=35.9%), OEF measured from ASE<sub>RF+</sub> was significantly higher (p=0.02), ASE<sub>RF-</sub> significantly lower (p<0.01), and VASO-ASE not significantly different (p=0.14), than TRUST OEF. Single-echo versions of ASE<sub>RF+</sub> (OEF=37.3±1.6%, median=37.1%, Q1=36.3%, Q3=38.6%) and ASE<sub>RF-</sub> (OEF=37.1±1.5% median=37.7%, Q1=36.6%, Q3=38.2%) were not significantly different, as expected (p=0.91). Boxplots with group-wise mean white matter results are shown in Figure 4, and additional statistical findings in Supporting Information Table S1. The range of TRUST-measured OEF values [range=15.9% (28.6-44.8%)] was greater than in the ASE variants [ASE<sub>RF+</sub> range=3.2% (24.0-27.2%), ASE<sub>RF-</sub> range=6.1% (34.1-40.2%), VASO-ASE range=8.5% (31.3-39.8%)].

### vCBV metrics

When considering dual-echo methods, ASE<sub>RF-</sub> yielded the highest vCBV measure (vCBV=10.8±1.4%; median=10.5%, Q1=10.0%, Q3=11.4%). vCBV values measured from ASE<sub>RF+</sub> (vCBV=5.0±0.5%; median=5.0%, Q1=4.6%, Q3=5.1%) and VASO-ASE (vCBV=3.8±0.5%; median=3.8%, Q1=3.4%, Q3=4.1%) were significantly lower (p<0.01) than ASE<sub>RF-</sub> vCBV values. When single echo variants were considered, ASE<sub>RF-</sub>

( $vCBV=5.0\pm 0.7\%$ ; median=4.8%, Q1=4.7%, Q3=5.1%) and  $ASE_{RF+}$  ( $vCBV=5.1\pm 0.5\%$ ; median=4.9%, Q1=4.7%, Q3=5.2%) were not significantly different ( $p=0.68$ ), as expected, and VASO-ASE yielded significantly lower ( $p<0.01$ )  $vCBV$  values.

## Discussion

Oxygen extraction fraction (OEF) measures from three variants of the asymmetric spin echo (ASE) pulse sequence were tested for repeatability and quantitative similarity to global OEF from  $T_2$ -Relaxation-Under-Spin-Tagging (TRUST), which has been validated against the historical gold-standard,  $^{15}O$  PET<sup>9,11</sup>. OEF values were most similar between the TRUST method and the novel VASO-ASE and  $ASE_{RF+}$  methods, which provided OEF in an expected physiological range. However, VASO-ASE provided a lower repeatability measure (ICC=0.61) compared to other methods (ICC 0.89).

Findings should be considered in light of commonly-accepted normal ranges of  $vCBV$  and OEF. Given a healthy white matter CBV of 0.02-0.03 ml blood / 100g tissue (2-3% voxel volume)<sup>33-35</sup>, and given that  $vCBV$  is approximately 70% of total CBV<sup>36</sup>, white matter  $vCBV$  which was analyzed here should be approximately 0.014-0.021 ml blood/100g tissue (1.4-2.1% voxel volume). VASO-ASE yielded values closer to this expected physiological range ( $vCBV=3.8\pm 0.5\%$ ), whereas  $ASE_{RF+}$  and  $ASE_{RF-}$  yielded higher estimates of  $vCBV$  ( $vCBV$  5.0%). As the ASE contrast model accounts for extravascular signal only, it is not surprising that, consistent with the primary study hypothesis, VASO-ASE yielded more physiologically plausible values than other methods without intravascular signal suppression. VASO-ASE and  $ASE_{RF+}$  OEF values were also more similar to TRUST and physiological expectation (OEF=31-44%)<sup>15</sup>, likely because the refocused readout reduces sensitivity to additional sources of susceptibility that may be magnified without second echo refocusing. We also considered two popular TRUST calibration models for completeness: one which was performed in bovine blood over a wide range of oxygenation values and healthy hematocrit values<sup>10</sup>, was utilized in a cross-modality validation study with PET<sup>11</sup>, and was observed to provide the most similar OEF values to those obtained from sinus measurements in catheterized piglets<sup>37</sup>. The other model utilized an abbreviated empirical calibration obtained from human blood<sup>31</sup>. Both models have been shown to provide similar OEF values over a range of normal hematocrit range in humans, and here we observed this as well with the full bovine model yielding values of  $32.7\pm 4.9\%$  and the empirical human model yielding values of  $36.5\pm 4.6\%$ . While the statistical significance of the findings between these two methods varied as expected, the overall trends of VASO-ASE (OEF=34.4 $\pm$ 2.3%) and  $ASE_{RF+}$  (OEF=36.8 $\pm$ 1.9%) providing values closer to TRUST, relative to  $ASE_{RF-}$  (26.1 $\pm$ 1.0%) were preserved regardless of model used.

The finding that TRUST reports a wider range of OEF values compared to ASE may partly be explained by the nature of the fitting and post-processing for ASE. Specifically, the ASE post-processing required spatial smoothing and averaging over large regions of white matter to compare with the global TRUST measure, however, the maps presented clearly show variation in OEF regionally (Figure 3). Additionally, OEF is inversely proportional to  $vCBV$ . Thus,  $vCBV$  overestimation in the first step of the fitting procedure reduces the OEF range.

Our findings support this, as when  $ASE_{RF+}$  and VASO-ASE methods are implemented, and  $vCBV$  values are lower, the range of reported OEF values becomes closer to that of TRUST.

Recent work has also demonstrated abilities to obtain more physiological OEF and  $vCBV$  values by using principles of inversion recovery to reduce the contributions from water outside of extravascular tissue compartments. For instance, Stone and Blockley introduced an inversion pre-pulse, in addition to other sequence improvements, timed to null the longitudinal component of the CSF magnetization in a combined qBOLD and ASE sequence<sup>17</sup>. The authors demonstrated that mean  $vCBV$  values reduced from  $4.7 \pm 0.7\%$  to a more physiological mean value of  $3.6 \pm 0.4\%$  ( $p < 0.001$ ) with the introduction of this module, and that the OEF reduced more slightly but significantly from  $23 \pm 2\%$  to  $21 \pm 2\%$  ( $p < 0.01$ ). Similar inversion recovery principles are applied in this study to improve model accuracy by suppressing the intravascular blood signal, and future work that incorporates both approaches, through double-inversion recovery or other principles, may further improve quantification accuracy across voxels that partial volume with CSF and blood.

Several challenges to routine VASO-ASE implementation should be addressed in future work.  $ASE_{RF+}$  outperformed VASO-ASE with regards to repeatability, likely owing to lower residual tissue magnetization, and corresponding SNR, for VASO-ASE. Additionally, slice-timing issues complicate multi-slice applications of VASO. These technical issues could be addressed with 3D readouts<sup>38,39</sup>, expanding contrast models, or by performing inflow VASO sequences that invert only inflowing blood water while leaving static tissue signal near equilibrium<sup>21,40</sup>. Favorably for ASE implementation, analysis of white matter OEF values measured from  $ASE_{RF-}$  and  $ASE_{RF+}$  demonstrated a moderate correlation (Pearson's  $r = 0.58$ ) between methods (Supporting Information Figure S2). This indicates that these two methods may be reporting on similar underlying physiology, and while  $ASE_{RF+}$  produces more physiological measures of OEF,  $ASE_{RF-}$  and previous studies which utilize it retain their value for understanding cerebral physiology. Additionally, intravascular  $T_2$  reduces more rapidly with increasing field strength compared to extravascular tissue  $T_2$ <sup>40,41</sup>, and as such similar echo times utilized at higher field strength (e.g., 7 Tesla) may be an additional option for suppressing intravascular signal in ASE, potentially obviating the need for inversion pre-pulses or bipolar gradients.

These findings should be regarded with several limitations. First, this study did not systematically investigate bipolar gradient strengths for nulling intravascular signal<sup>8</sup>. However, it is worth noting that this method increases TE, is incompletely effective depending on b-value choice, and can be dependent on vessel orientation and gradient scheme. Second, while OEF values are compared between TRUST and ASE, TRUST is a whole-brain measure of OEF, while ASE values in this study were calculated in white matter. The motivation for this choice was to reduce CSF partial-volume effects in ASE voxels where the extravascular tissue model was inaccurate. Third, while VASO-ASE is novel and gives further insight into the relationship between intravascular signal and calculated physiological parameters, due to timing issues this method is limited to one echo and one slice. Concerns regarding comparison of single-slice VASO-ASE to multi-slice methods are addressed in Supporting Information Figure S3 and Figure 4 (d-f), which demonstrate that expected relationships between VASO-ASE and other methods



are preserved when matching slices and echoes between methods. Fourth, we did not specifically evaluate field heterogeneity or blood water nulling accuracy in this study. However, the slices compared were identical across all ASE modalities and at a fronto-parietal level where  $B_0$  and  $B_1$  homogeneity is high. Additionally, we utilized blood water nulling times nearly identical to those investigated in prior VASO studies using identical body coil blood water adiabatic inversion<sup>42,43</sup>. While it is unlikely that performance would differ significantly in the present study, this was not investigated rigorously here.

In conclusion, we measured three variants of the asymmetric spin echo pulse sequence, two of which are novel and designed to bring acquired data into correspondence with extravascular tissue models<sup>27</sup>. We observed that VASO-ASE and refocused dual-echo ASE provide OEF values most similar to global OEF acquired from TRUST. Future work that extends these methods to improve spatial coverage, signal-to-noise ratio, and repeatability are warranted.

## Supplementary Material

Refer to Web version on PubMed Central for supplementary material.

## Acknowledgements

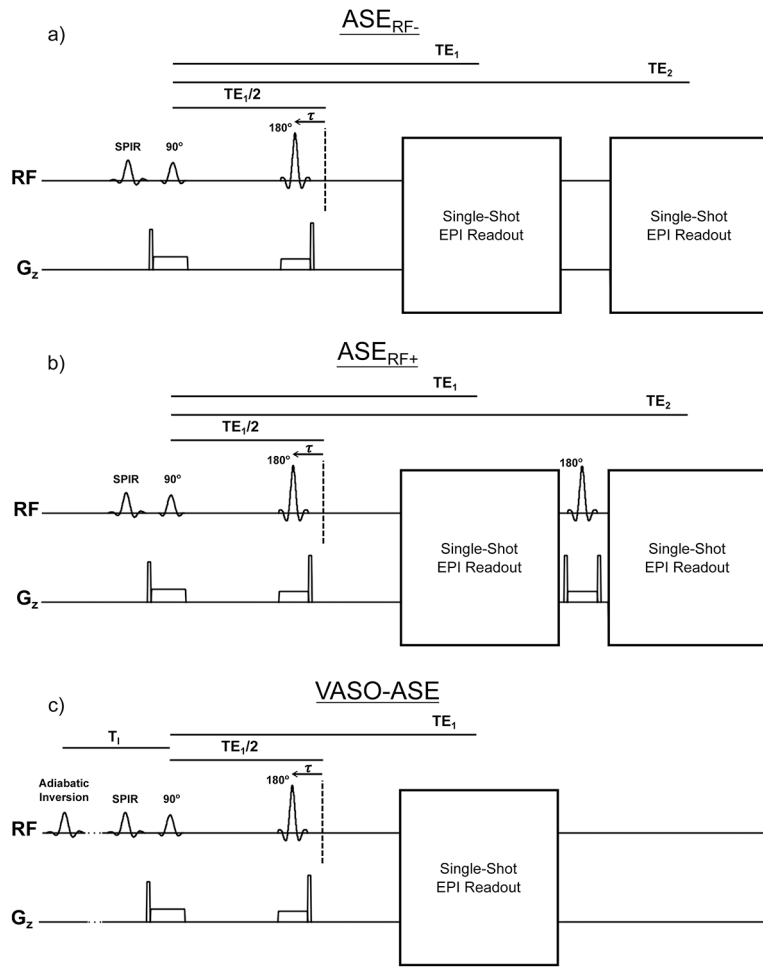
Funding: NIH/NINDS 5R01NS097763.

## References

1. Powers WJ, Grubb RL Jr., Darriet D, Raichle ME. Cerebral blood flow and cerebral metabolic rate of oxygen requirements for cerebral function and viability in humans. *J Cereb Blood Flow Metab.* 1985;5(4):600–608. [PubMed: 3877067]
2. Powers WJ, Clarke WR, Grubb RL, Jr., et al. Extracranial-intracranial bypass surgery for stroke prevention in hemodynamic cerebral ischemia: the Carotid Occlusion Surgery Study randomized trial. *JAMA.* 2011;306(18):1983–1992. [PubMed: 22068990]
3. Lin W, Powers WJ. Oxygen metabolism in acute ischemic stroke. *J Cereb Blood Flow Metab.* 2018;38(9):1481–1499. [PubMed: 28792276]
4. Jiang D, Lu H. Cerebral oxygen extraction fraction MRI: Techniques and applications. *Magn Reson Med.* 2022;88(2):575–600. [PubMed: 35510696]
5. Derdeyn CP, Videen TO, Grubb RL, Jr., Powers WJ. Comparison of PET oxygen extraction fraction methods for the prediction of stroke risk. *J Nucl Med.* 2001;42(8):1195–1197. [PubMed: 11483680]
6. Ter-Pogossian MM, Eichling JO, Davis DO, Welch MJ. The measure in vivo of regional cerebral oxygen utilization by means of oxyhemoglobin labeled with radioactive oxygen-15. *J Clin Invest.* 1970;49(2):381–391. [PubMed: 5411789]
7. Lu H, Ge Y. Quantitative evaluation of oxygenation in venous vessels using T2-Relaxation-Under-Spin-Tagging MRI. *Magn Reson Med.* 2008;60(2):357–363. [PubMed: 18666116]
8. An H, Lin W. Impact of intravascular signal on quantitative measures of cerebral oxygen extraction and blood volume under normo- and hypercapnic conditions using an asymmetric spin echo approach. *Magn Reson Med.* 2003;50(4):708–716. [PubMed: 14523956]
9. Liu P, Xu F, Lu H. Test-retest reproducibility of a rapid method to measure brain oxygen metabolism. *Magn Reson Med.* 2013;69(3):675–681. [PubMed: 22517498]
10. Lu H, Xu F, Grgac K, Liu P, Qin Q, van Zijl P. Calibration and validation of TRUST MRI for the estimation of cerebral blood oxygenation. *Magn Reson Med.* 2012;67(1):42–49. [PubMed: 21590721]

11. Jiang D, Deng S, Franklin CG, et al. Validation of T2 -based oxygen extraction fraction measurement with (15) O positron emission tomography. *Magn Reson Med.* 2021;85(1):290–297. [PubMed: 32643207]
12. Qi Y, Liu P, Lin Z, Lu H, Wang X. Hemodynamic and Metabolic Assessment of Neonates With Punctate White Matter Lesions Using Phase-Contrast MRI and T2-Relaxation-Under-Spin-Tagging (TRUST) MRI. *Front Physiol.* 2018;9:233. [PubMed: 29615927]
13. Morris EA, Juttukonda MR, Lee CA, et al. Elevated brain oxygen extraction fraction in preterm newborns with anemia measured using noninvasive MRI. *J Perinatol.* 2018.
14. Jiang D, Lin Z, Liu P, et al. Brain Oxygen Extraction Is Differentially Altered by Alzheimer’s and Vascular Diseases. *J Magn Reson Imaging.* 2020;52(6):1829–1837. [PubMed: 32567195]
15. Donahue MJ, Achten E, Cogswell PM, et al. Consensus statement on current and emerging methods for the diagnosis and evaluation of cerebrovascular disease. *J Cereb Blood Flow Metab.* 2017;271678X17721830.
16. Stone AJ, Holland NC, Berman AJL, Blockley NP. Simulations of the effect of diffusion on asymmetric spin echo based quantitative BOLD: An investigation of the origin of deoxygenated blood volume overestimation. *Neuroimage.* 2019;201:116035. [PubMed: 31326570]
17. Stone AJ, Blockley NP. A streamlined acquisition for mapping baseline brain oxygenation using quantitative BOLD. *Neuroimage.* 2017;147:79–88. [PubMed: 27915118]
18. Donahue MJ, Sideso E, MacIntosh BJ, Kennedy J, Handa A, Jezzard P. Absolute arterial cerebral blood volume quantification using inflow vascular-space-occupancy with dynamic subtraction magnetic resonance imaging. *J Cereb Blood Flow Metab.* 2010;30(7):1329–1342. [PubMed: 20145656]
19. Lu H, Golay X, Pekar JJ, Van Zijl PC. Functional magnetic resonance imaging based on changes in vascular space occupancy. *Magn Reson Med.* 2003;50(2):263–274. [PubMed: 12876702]
20. Huber LR, Poser BA, Kaas AL, et al. Validating layer-specific VASO across species. *Neuroimage.* 2021;237:118195. [PubMed: 34038769]
21. Cheng Y, Qin Q, van Zijl PCM, Pekar JJ, Hua J. A three-dimensional single-scan approach for the measurement of changes in cerebral blood volume, blood flow, and blood oxygenation-weighted signals during functional stimulation. *Neuroimage.* 2017;147:976–984. [PubMed: 28041979]
22. Wang Y, Guilliams KP, Fields ME, et al. Silent Infarcts, White Matter Integrity, and Oxygen Metabolic Stress in Young Adults With and Without Sickle Cell Trait. *Stroke.* 2022;101161STROKEAHA121036567.
23. Guilliams KP, Fields ME, Ragan DK, et al. Red cell exchange transfusions lower cerebral blood flow and oxygen extraction fraction in pediatric sickle cell anemia. *Blood.* 2018;131(9):1012–1021. [PubMed: 29255068]
24. Kang P, Ying C, Chen Y, Ford AL, An H, Lee JM. Oxygen Metabolic Stress and White Matter Injury in Patients With Cerebral Small Vessel Disease. *Stroke.* 2022;53(5):1570–1579. [PubMed: 34886686]
25. Lu H, Clingman C, Golay X, van Zijl PC. Determining the longitudinal relaxation time (T1) of blood at 3.0 Tesla. *Magn Reson Med.* 2004;52(3):679–682. [PubMed: 15334591]
26. An H, Lin W. Cerebral oxygen extraction fraction and cerebral venous blood volume measurements using MRI: effects of magnetic field variation. *Magn Reson Med.* 2002;47(5):958–966. [PubMed: 11979575]
27. Yablonskiy DA, Haacke EM. Theory of NMR signal behavior in magnetically inhomogeneous tissues: the static dephasing regime. *Magn Reson Med.* 1994;32(6):749–763. [PubMed: 7869897]
28. Weisskoff RM, Kiihne S. MRI susceptometry: image-based measurement of absolute susceptibility of MR contrast agents and human blood. *Magn Reson Med.* 1992;24(2):375–383. [PubMed: 1569876]
29. Woolrich MW, Jbabdi S, Patenaude B, et al. Bayesian analysis of neuroimaging data in FSL. *Neuroimage.* 2009;45(1 Suppl):S173–186. [PubMed: 19059349]
30. Jordan LC, Gindville MC, Scott AO, et al. Non-invasive imaging of oxygen extraction fraction in adults with sickle cell anaemia. *Brain.* 2016;139(Pt 3):738–750. [PubMed: 26823369]
31. Bush A, Borzage M, Detterich J, et al. Empirical model of human blood transverse relaxation at 3 T improves MRI T2 oximetry. *Magn Reson Med.* 2017;77(6):2364–2371. [PubMed: 27385283]

32. Koo TK, Li MY. A Guideline of Selecting and Reporting Intraclass Correlation Coefficients for Reliability Research. *J Chiropr Med*. 2016;15(2):155–163. [PubMed: 27330520]
33. Leggett RW, Williams LR. Suggested reference values for regional blood volumes in humans. *Health Phys*. 1991;60(2):139–154. [PubMed: 1989937]
34. Sakai F, Nakazawa K, Tazaki Y, et al. Regional cerebral blood volume and hematocrit measured in normal human volunteers by single-photon emission computed tomography. *J Cereb Blood Flow Metab*. 1985;5(2):207–213. [PubMed: 3921557]
35. Lin W, Paczynski RP, Kuppusamy K, Hsu CY, Haacke EM. Quantitative measurements of regional cerebral blood volume using MRI in rats: effects of arterial carbon dioxide tension and mannitol. *Magn Reson Med*. 1997;38(3):420–428. [PubMed: 9339444]
36. Hua J, Liu P, Kim T, et al. MRI techniques to measure arterial and venous cerebral blood volume. *Neuroimage*. 2019;187:17–31. [PubMed: 29458187]
37. Liu D, Jiang D, Tekes A, et al. Multi-Parametric Evaluation of Cerebral Hemodynamics in Neonatal Piglets Using Non-Contrast-Enhanced Magnetic Resonance Imaging Methods. *J Magn Reson Imaging*. 2021;54(4):1053–1065. [PubMed: 33955613]
38. Donahue MJ, Blicher JU, Ostergaard L, et al. Cerebral blood flow, blood volume, and oxygen metabolism dynamics in human visual and motor cortex as measured by whole-brain multi-modal magnetic resonance imaging. *J Cereb Blood Flow Metab*. 2009;29(11):1856–1866. [PubMed: 19654592]
39. Poser BA, Norris DG. 3D single-shot VASO using a Maxwell gradient compensated GRASE sequence. *Magn Reson Med*. 2009;62(1):255–262. [PubMed: 19319900]
40. Donahue MJ, Hoogduin H, van Zijl PC, Jezzard P, Luijten PR, Hendrikse J. Blood oxygenation level-dependent (BOLD) total and extravascular signal changes and  $\Delta R_2^*$  in human visual cortex at 1.5, 3.0 and 7.0 T. *NMR Biomed*. 2011;24(1):25–34. [PubMed: 21259367]
41. Duong TQ, Yacoub E, Adriany G, Hu X, Ugurbil K, Kim SG. Microvascular BOLD contribution at 4 and 7 T in the human brain: gradient-echo and spin-echo fMRI with suppression of blood effects. *Magn Reson Med*. 2003;49(6):1019–1027. [PubMed: 12768579]
42. Donahue MJ, Lu H, Jones CK, Edden RA, Pekar JJ, van Zijl PC. Theoretical and experimental investigation of the VASO contrast mechanism. *Magn Reson Med*. 2006;56(6):1261–1273. [PubMed: 17075857]
43. Donahue MJ, Hua J, Pekar JJ, van Zijl PC. Effect of inflow of fresh blood on vascular-space-occupancy (VASO) contrast. *Magn Reson Med*. 2009;61(2):473–480. [PubMed: 19161167]

**Figure 1.**

All pulse sequences for the asymmetric spin echo (ASE) that are investigated in this study. Spatial resolution =  $3.44 \times 3.44 \times 3.00$  mm, Repetition time (TR)=4400ms and first echo time ( $TE_1$ )=64 ms were common for all approaches. For dual-echo sequences, the second echo ( $TE_2$ ) was 107 ms. For vascular space occupancy ASE (VASO-ASE),  $TI=1039$ ms, the inversion time for nulling the steady-state longitudinal component of the blood water magnetization at the prescribed TR=4400 ms. Non-refocused dual-echo ASE ( $ASE_{RF-}$ ) is shown in a) and is a common method for implementing ASE in clinical applications. Refocused dual-echo ASE ( $ASE_{RF+}$ ) is shown in b) and adds a refocusing pulse between the first and second readout in ASE. Vascular space occupancy ASE (VASO-ASE) is shown in c) and adds an intravascular signal nulling pre-pulse to null intravascular blood water. Due to slice timing constraints and signal loss caused by the VASO pre-pulse, VASO-ASE is single slice and single-echo, while all other methods have two echoes and 13 slices.

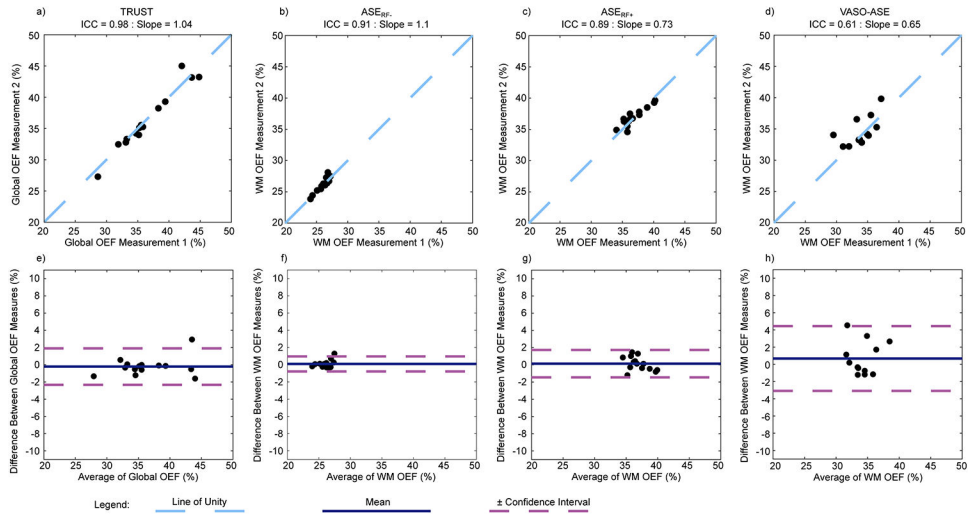


**Figure 2.**

Regression and Bland-Altman Plots for repeatability of T2-relaxation-under-spin-tagging (TRUST), and asymmetric spin echo (ASE) variants: ASE<sub>RF-</sub>, ASE<sub>RF+</sub>, and VASO-ASE (see Figure 1 for description). Repeatability (measured as intraclass correlation coefficient, ICC) is excellent for TRUST (ICC=0.98), ASE<sub>RF-</sub> (ICC=0.91), and ASE<sub>RF+</sub> (ICC=0.89), but moderate for VASO-ASE (ICC=0.61). Purple lines denote the 95% confidence interval on Bland-Altman analysis.

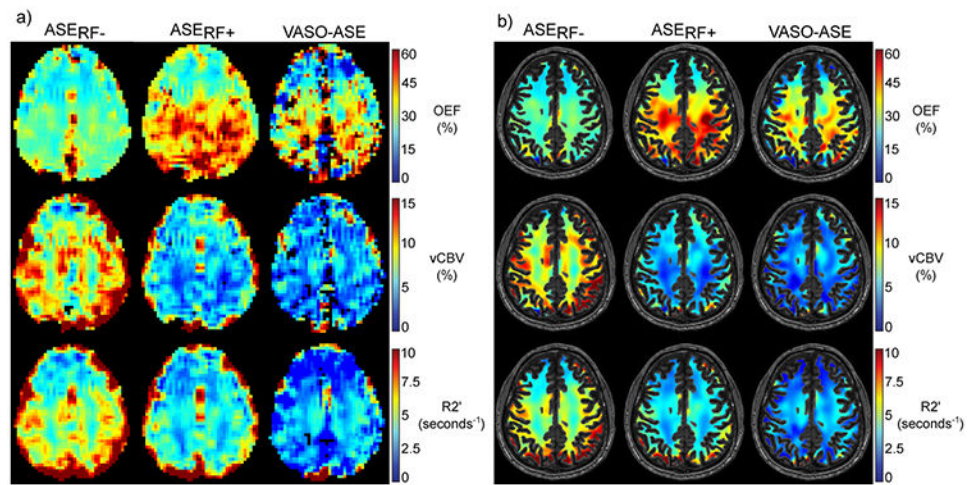


**Figure 3.**

Representative images for each physiological parameter map calculated from asymmetric spin echo (ASE) and each ASE variant are shown in a) and b). The unmasked and white matter (WM) masked images are shown separately (see Methods for additional processing details). Oxygen extraction fraction (OEF) is higher in posterior territories compared to anterior territories due to susceptibility effects originating from air-tissue interface effects in the sinuses.

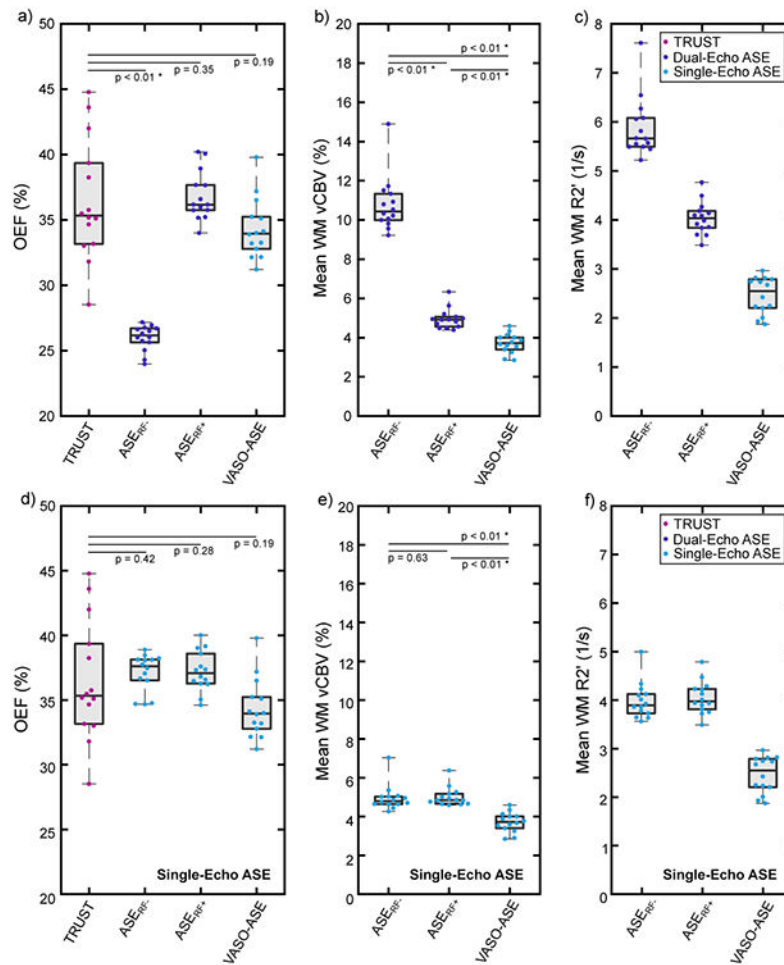


**Figure 4.**

Panels a-c show quantified values for T2-relaxation-under-spin-tagging (TRUST) and all asymmetric spin echo (ASE) variants investigated in this study using both echoes for quantification in the ASE sequences, with the exception of VASO-ASE, which is a single-echo sequence (see Figure 1). The ASE<sub>RF+</sub> and VASO-ASE variants yielded oxygen extraction fraction (OEF) values most similar to TRUST OEF values, and these variants also yielded venous cerebral blood volume (vCBV) values closer to physiological expectation. Panels d-f exclude the second echo for dual-echo ASE variants. Note that with the exclusion of the second echo, ASE<sub>RF+</sub> and ASE<sub>RF-</sub> are identical sequences. These plots demonstrate that the second echo affects the results from ASE<sub>RF-</sub>, but not for ASE<sub>RF+</sub>. VASO-ASE is already a single-echo method, and is therefore unaffected. When excluding the second echo for dual-echo approaches, the finding that VASO-ASE produces the lowest vCBV values, which are closest to physiological expectation, is preserved. Quantified values are shown in Table 1.

**Table 1.**

Demographic information for all 14 participants of this study. Continuous parameters are presented as mean  $\pm$  standard deviation. Asymmetric spin echo (ASE) values shown are for the dual-echo approach; single-echo values are summarized in Figure 4. Abbreviations: T2-relaxation-under-spin-tagging (TRUST), oxygen extraction fraction (OEF), venous cerebral volume (vCBV), Vascular space occupancy (VASO).

Parameter	Value
<i>Demographic</i>	
Number of participants	14
Age	28 $\pm$ 5 years
Race (White / Asian / Black)	11 / 2 / 1
Fraction participants male / female	0.50 / 0.50
<i>Oxygen extraction fraction (OEF)</i>	
TRUST, HbAA model	36.5 $\pm$ 4.6%
TRUST, Bovine model	32.7 $\pm$ 4.9%
ASE <sub>RF-</sub>	26.1 $\pm$ 1.0%
ASE <sub>RF+</sub>	36.8 $\pm$ 1.9%
VASO-ASE	34.4 $\pm$ 2.3%
<i>Venous cerebral blood volume (vCBV)</i>	
ASE <sub>RF-</sub> -vCBV	10.8 $\pm$ 1.4%
ASE <sub>RF+</sub> -vCBV	5.0 $\pm$ 0.5%
VASO-ASE-vCBV	3.8 $\pm$ 0.5%